BIOCHEMISTRY
including biophysical chemistry & molecular biology

Article

pubs.acs.org/biochemistry

Accessibility and External versus Intercalative Binding to DNA As Assessed by Oxygen-Induced Quenching of the Palladium(II)-Containing Cationic Porphyrins Pd(T4) and Pd(*t*D4)

Matthew A. Bork,[†] Christopher G. Gianopoulos,[†] Hanyu Zhang,[‡] Phillip E. Fanwick,[†] Jong Hyun Choi,[‡] and David R. McMillin*[,†]

[†]Department of Chemistry, Purdue University, 560 Oval Drive, West Lafayette, Indiana 47907, United States

[‡]School of Mechanical Engineering, Purdue University, West Lafayette, Indiana 47907, United States

Supporting Information

ABSTRACT: Studies reveal that it is possible to design a palladium(II)-containing porphyrin to bind exclusively by intercalation to double-stranded DNA while simultaneously enhancing the ability to sensitize the formation of singlet oxygen. The comparisons revolve around the cations [5,10,15,20-tetra(*N*-methylpyridinium-4-yl)porphyrin]palladium(II), or Pd(T4), and [5,15-di(*N*-methylpyridinium-4-yl)porphyrin]palladium(II), or Pd(*t*D4), in conjunction with A═T and G≡C rich DNA binding sequences. Methods employed include X-ray crystallography of the ligands as well as absorbance, circular dichroism, and emission spectroscopies of the adducts and the emission from singlet oxygen in solution. In the case of the bulky Pd(T4) system, external binding is almost as effective as intercalation in slowing the rate of oxygen-induced quenching of the porphyrin's triplet excited state. The fractional efficiency of quenching by oxygen nevertheless approaches 1 for intercalated forms of Pd(*t*D4), because of intrinsically long triplet lifetimes. The intensity of the sensitized, steady-state emission signal varies with the system and depends on many factors, but the Pd(*t*D4) system is impressive. Intercalated forms of Pd(*t*D4) produce higher sensitized emission yields than Pd(T4) is capable of in the absence of DNA.

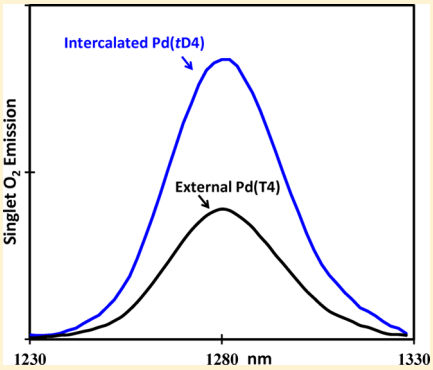

More than 30 years ago, Fiel and co-workers reported seminal work on the DNA binding interactions of water-soluble, cationic porphyrins.[1] Scheme 1 includes structures of two of the originally studied systems, H_2T4 and H_2TMAP, or 5,10,15,20-tetra(*N*-methylpyridinium-4-yl)porphyrin and 5,10,15,20-tetra(*N*,*N*,*N*-trimethylanilinium-4-yl)porphyrin, respectively. A large number of investigations have followed,[2−4] driven in part by the potential for therapeutic uses. For example, the ligands are applicable as sensitizers for photodynamic therapy, or PDT, because of the strong absorption the chromophore exhibits in the long wavelength end of the visible spectrum.[5−8] Potential applications extend to antibactericidal action in support of wound healing as well as antivirus therapy.[9,10] A nonphotochemistry-related application arises from the fact that cationic porphyrins effectively inhibit telomerase, an enzyme implicated in the immortalization of cancer cells.[11−13]

Cellular DNA is an attractive target in most if not all of the applications mentioned, and a cationic porphyrin can adopt a number of binding motifs. Aggregation-based, outside binding is a possibility for porphyrins like H_2TMAP, which is inherently prone to self-stacking in aqueous solution.[14,15] However, aggregation leads to excited-state lifetimes that are too short for conventional PDT. In terms of monomer binding, the Fiel group found that H_2T4 was better behaved but exhibited two distinct binding motifs.[14,16] Subsequent studies have indeed confirmed that H_2T4 intercalates into double-stranded (ds) DNA sequences if they are rich in guanine-cytosine (G≡C) base pairs, while it binds externally to sequences that are rich in adenine-thymine (A═T) base pairs.[3,4] In the simplest of terms, the steric properties of the ligand and the rigidity of the DNA host combine to determine which binding motif is more favorable.[17] The bulkiness of the H_2T4 framework derives from the four, out-of-plane pyridiniumyl substituents.[1] Incorporating a central metal that requires axial ligands introduces even more steric constraints and precludes ordinary intercalative binding, regardless of the base sequence.[15,18,19] On the other hand, nonaxially ligated forms like Pd(T4) and Cu(T4) tend to show the same binding preferences as H_2T4.[3] For intercalated Cu(T4), structural studies by Williams and co-workers suggest that the major steric issues arise in the minor groove where a pair of ligand substituents clash with sugar−phosphate backbone residues of the host.[20] Marzilli and co-workers have recently summarized many studies aimed at understanding how the extension, average charge, and/or size of the peripheral substituents impacts the choice of binding motif.[15] An

Received: December 3, 2013
Revised: January 11, 2014
Published: January 15, 2014

   dx.doi.org/10.1021/bi401610t | *Biochemistry* 2014, 53, 714−724

Scheme 1

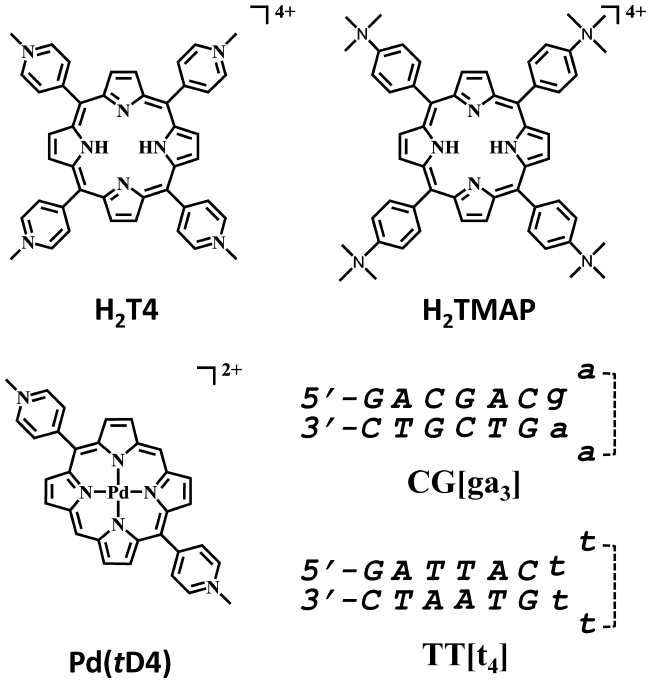

alternative strategy is to reduce the number of substituents. Indeed, recent studies have established that intercalation becomes the sole binding motif for appropriate di- and trisubstituted forms interacting with ds DNA.[21−25]

Designing porphyrins that bind to ds DNA in a predictable fashion is a fundamental challenge and a very worthy pursuit if it promotes a useful end. A logical approach is to shape porphyrins to be effective intercalators, because insertion into the stack of DNA bases has a favorable hydrophobic effect and preserves Watson−Crick hydrogen bonding within the host. However, the other side of the coin is that internalization may be incompatible with the goal of sensitizing singlet oxygen, if the DNA framework too completely blocks contact with the O_2 molecule in solution. To assess sensitization issues, the following studies center on palladium(II)-containing porphyrins because they exhibit relatively long triplet excited-state lifetimes.[26] The model hosts are two hairpin-forming sequences, previously demonstrated to be convenient vehicles for studying DNA binding interactions.[17,23,27] One of the hosts presents a double-stranded stem rich in A═T base pairs, while the other incorporates a G≡C rich stem. As expected, the bulky porphyrin Pd(T4) intercalates into the latter and binds externally to the former. External binding proves to be almost as effective as intercalation at shrouding the porphyrin. At the same time, oxygen-induced quenching proves to be uniformly efficient and markedly so in the case of the sterically friendly Pd(*t*D4) system, which binds exclusively by intercalation.

EXPERIMENTAL PROCEDURES

Materials. The provider of commercial paraformaldehyde, NaOH, hexanes, dichloromethane (DCM), chloroform, dimethylformamide (DMF), pyridine, acetone, methanol (MeOH), acetonitrile (MeCN), and isopropyl alcohol was Mallinckrodt Chemicals. Macron Chemicals supplied acetic acid and nitric acid, while the source of hydrochloric acid was J. T. Baker. The silica was a product of Sorbent Technologies. EMD Chemicals and Integrated DNA Technologies were the sources for triethylamine (98%) and the DNA sequences, respectively. Indium(III) chloride, Trizma HNO_3 buffer, Trizma base, pyrrole, pyridine-4-carboxaldehyde, tetrabutylammonium nitrate, tetrabutylammonium *p*-toluenesulfonate, potassium hexafluorophosphate, sodium nitrate, methyl iodide, silica TLC plates, fluorisil, acetonitrile, silanizing solutions, potassium tetrachloroplatinate, and potassium tetrachloropalladate were from Sigma-Aldrich Commercial, as was the *p*-toluene sulfonate (PTS or tosylate) salt of H_2T4. The latter was the only commercial product subjected to a purification procedure (*vide infra*). Cambridge Isotopes Laboratory, Inc., supplied isotopically enriched D_2O and d_4-MeOH for emission studies involving singlet oxygen.

Methods. The syntheses of the three metalloporphyrins were all multistep processes. To minimize photodecomposition, synthesis and purification steps were conducted in diffuse lighting. Galbraith Laboratories, Inc. (Nashville, TN), or Midwest Microlab, LLC (Indianapolis, IN), conducted all microanalyses.

Tosylate Salt of Pd(tD4). The synthesis of the dipyrromethane (dpm) precursor was a variation on a literature method in which pyrrole serves as the solvent.[28] After reaction, removal of the indium catalyst, and evaporation of the excess pyrrole, it was possible to extract dpm into hot hexane, from which dpm deposited as a white solid.[22] The combination of dpm with pyridine-4-carboxaldehyde yielded the neutral porphyrin *trans*-5,15-(dipyrid-4-yl)porphyrin (H_2*t*D4n) via a published procedure.[22] Exposing H_2*t*D4n to excess methyl iodide in DMF at 50 °C induced methylation of the pyridine nitrogens but typically resulted in a mixture of products. Separation could be achieved by chromatography on SiO_2 (previously treated with 2% triethylamine in water). After the solution containing the crude product had been loaded, elution with DCM removed neutral compounds. The next mobile phase used was a 50:50 MeCN/water mixture. Subsequently, a solution containing 80% acetonitrile, 10% saturated KNO_3(aq), and 10% water eluted singly methylated porphyrin. Another elution with a 50:50 MeCN/water mixture removed salts before elution with 0.01 M HCl in a 50:50 water/MeCN mixture yielded fractions containing dicationic porphyrin. [The HCl treatment presumably also removes any adventitious Zn(II) bound to the porphyrin.] After the evaporation of acetonitrile, addition of KPF_6(aq) precipitates the porphyrin. Ion exchange to the *p*-toluene sulfonate (PTS), or tosylate salt, can be achieved by dissolving the hexafluorophosphate salt in acetonitrile and precipitating with a solution of tetrabutylammonium tosylate in acetone.

The formation of Pd(*t*D4) occurs in aqueous solution. Pretreating all glassware with acid helps reduce the level of kinetically favorable incorporation of adventitious zinc(II). In the first step, a published method yields the palladium-containing intermediate, $Pd(DMSO)_2Cl_2$, from commercially available $PdCl_2$.[29,30] Subsequent modification involves treating an aqueous suspension of $Pd(DMSO)_2Cl_2$ with ∼1.6 equiv of $AgNO_3$(aq) at 0 °C and removing AgCl(s) by centrifugation and filtration.[31] Metalation of the porphyrin proceeds upon combining the soluble palladium precursor with the tosylate salt of H_2*t*D4 and refluxing for ∼2 days. The total amount of Pd(II) added is ∼10 equiv, introduced over a period of hours in three equal aliquots. After reaction, the addition of excess KPF_6(aq) induces precipitation of the product. Simple metathesis permits exchange of the anion to either the tosylate or nitrate form. Pure crystals of the tosylate salt deposit with

dx.doi.org/10.1021/bi401610t | *Biochemistry* 2014, 53, 714−724

slow evaporation of a mixed solvent originally consisting of a 2:1 methanol/2-propanol mixture. Anal. Calcd for $C_{32}H_{24}N_6Pd{\cdot}2(C_7H_7O_3S){\cdot}CH_3OH{\cdot}0.5H_2O$: C, 57.47; H, 4.41; N, 8.55. Found: C, 57.23; H, 4.27; N, 8.34.

Nitrate Salt of Pd(T4). The first step involves purification of the ligand. Commercially obtained H_2T4 nominally includes a tetramethylated cationic porphyrin, but thin-layer chromatography (TLC) reveals the material contains the three-plus form, as well.[32] However, heating at 50 °C in DMF containing excess methyl iodide converts all the porphyrin to the chromatographically pure, tetracationic state. Addition of tetrabutylammonium nitrate in acetone induces precipitation of the porphyrin. Dissolving the product in water and treating with dilute HCl(aq) induced loss of adventitious zinc(II) before reprecipitating by addition of KPF_6(aq). One last ion exchange involves dissolving the hexafluorophosphate form in acetonitrile and precipitating the nitrate form by addition of tetrabutylammonium nitrate in acetone.

Once again, water is the solvent of choice for inserting palladium. Refluxing the nitrate form of the porphyrin with $Pd(DMSO)_2Cl_2$, solubilized as before by pretreatment with $AgNO_3$(aq), effected insertion of palladium(II). The addition of excess KPF_6(aq) induced precipitation of the hexafluorophosphate salt. Simple metathesis permits exchange of the anion to either the tosylate or nitrate form. Slow diffusion of ether into a methanol solution of the latter produced analytically pure crystals. Anal. Calcd for $C_{72}H_{64}N_8O_{12}Pd{\cdot}4(PTS){\cdot}2.5\ H_2O$: C, 57.16; H, 4.59; N, 7.41. Found: C, 57.06; H, 4.21; N, 7.51.

Nitrate Salt of Pt(T4). A similar treatment of $Pt(DMSO)_2Cl_2$ with $AgNO_3$(aq), except at room temperature, produced a water-soluble platinum precursor.[31] Refluxing a solution of the nitrate salt of H_2T4 in water in the dark with 4 equiv of Pt(II), added in three aliquots, promoted insertion of platinum. The reaction time was ~6 days. After reaction, the addition of KPF_6(aq) induced precipitation of the product. Metathesis with tetrabutylammonium nitrate in acetone yields the corresponding nitrate salt of Pt(T4). Absorbance and emission data showed the crude product contained H_2T4 and Zn(T4) as contaminants. It is possible to remove both by dissolving the nitrate form in water, adding HCl(aq), and inducing fractional precipitation by addition of KPF_6(aq). The acid treatment induces dissociation of Zn(II) along with the protonation of the inner nitrogens of H_2T4 as evidenced by the change in color from deep red to green. Preferential deposition of Pt(T4) as the hexafluorophosphate salt by careful addition of KPF_6(aq) leads to a pure product. Exchange of the counterion can occur via simple metathesis. Slow evaporation of an aqueous solution of the nitrate form yielded crystals suitable for crystallographic analysis.

Glassware Treatment. The measures necessary depend on the procedure. For porphyrin synthesis, the treatment involves filling the vessel with a 50:50 mixture of nitric acid and hydrochloric acid to strip zinc(II) ions adsorbed to the inner walls. After overnight exposure, washing multiple times with deionized water and, if appropriate, organic solvent effectively removed excess acid. Conditioning for DNA binding studies requires subsequent exposure to a silanizing agent.[33]

Buffer Preparation. The aqueous buffer used in the binding studies was 0.01 M in Tris-nitrate. Adjustment to pH 7.5 was possible with the addition of Tris base. The addition of $NaNO_3$(s) achieved the final ionic strength (μ) of 0.05. The storage temperature was ~5 °C in a laboratory refrigerator.

DNA Binding Studies. The binding studies followed published procedures.[23] To avoid aggregation of the porphyrin, the medium used for measuring spectra of Pd(*t*D4) contained 50% Tris buffer and 50% MeOH, unless DNA host was present.[34] When DNA is present in the sample, the only source of MeOH is a small amount introduced with the porphyrin stock solution, which is 50% MeOH by volume. By also introducing additional porphyrin along with each aliquot of DNA stock solution, we were able to maintain the porphyrin concentration constant as *q*, the DNA base pair:porphyrin concentration ratio, varies. The path length of cuvettes used for emission measurements was always 1.0 cm, but the absorbance at the excitation wavelength generally changes during titrations. Dividing the emission intensity at each wavelength λ by the fraction of light absorbed ($1 - 10^{-A'}$), where A' denotes the absorbance at the excitation wavelength, effectively compensates for absorbance differences and facilitates comparisons between runs.[35] Multiplying the raw circular dichroism (CD) signals (in millidegrees) by $(Qcl)^{-1}$, where Q equals 32980, c is the molar concentration of the chromophore, and l is the path length in centimeters, converts the scale to a $\Delta\varepsilon$ basis. Further treatment of data involves subtracting the baseline obtained in a buffer-only run and averaging the signals obtained between 475 and 500 nm to correct for any net offset from zero. Equation 1 allows calculation of the percent hypochromism (% H), where $A(\lambda)$ is the absorption at the Soret maximum of the free porphyrin and $A(\lambda')$ is the maximal absorption by the bound porphyrin, which occurs at λ', because of the bathochromic response.

$$\%H = \frac{A(\lambda) - A(\lambda')}{A(\lambda)} \times 100 \quad (1)$$

The concentration of porphyrin was always 2.0 μM. In conjunction with Beer's law, absorbance measurements and the molar extinction coefficients allowed calculations of concentrations of all stock solutions. Spectrophotometric titrations involved addition of DNA, usually in steps of 8 bp per unit of porphyrin. The hairpin-forming DNA sequences used were 5′-GA**TT**ACttttGTAATC-3′ (TT[t_4]) and 5′-GA**CG**ACgaaaGTCGTC-3′ (CG[ga_3]), where lowercase letters designate bases involved in loop formation. The abbreviated names derive from the one-letter codes of the variable bases that appear in bold type and reside at positions 3 and 4, amidst the double-stranded stem of the folded hairpin. The molar extinction coefficients[27] for the UV absorptions of the latter are 17150 M^{-1} cm^{-1} (TT[t_4]) and 18125 M^{-1} cm^{-1} (CG[ga_3]).

Luminescence Measurements. For emission spectra, the slit settings for excitation and emission were 10 nm. Long pass filters of the appropriate wavelength shielded the detector from scattering of the excitation beam. Manufacturer-supplied factors allowed for correcting spectra for changes in detector sensitivity as a function of wavelength. Use of a variable delay, variable gate app, supplied by Cary, was necessary to obtain accurate emission intensities because of the long lifetimes of the emissions from the palladium-containing porphyrins.

The method of Parker and Rees provided estimates of emission quantum yields, with the $[Ru(bpy)_3]^{2+}$ complex dissolved in acetonitrile as a standard (ϕ = 0.062).[36,37] The criterion for the choice of the wavelength of excitation was that both the sample and standard have the same absorbance. Equation 2 provided estimates of the quantum yields:

Table 1. Crystal Data

molecular formula	$C_{32}H_{24}N_6Pd{\cdot}2(C_7H_7O_3S){\cdot}CH_3OH$	$C_{44}H_{36}N_8Pt{\cdot}4(H_2O){\cdot}4(NO_3)$
Fw	973.42	1192.00
space group	$P121/c1$ (No. 14)	$P2_1/n$ (No. 14)
a (Å)	27.7639(8)	5.5001(3)
b (Å)	8.8237(2)	28.6745(13)
c (Å)	17.4114(3)	14.9953(11)
β (deg)	105.262(10)	96.75(5)
V	4115.02(17)	2348.6(2)
Z	4	2
ρ_{calc} (g/cm^3)	1.571	1.685
μ (mm^{-1})	0.616	6.355
transmission coefficient	0.817−0.955	0.598−0.683
T (K)	150	150
no. of reflections measured	23037	18932
no. of independent reflections	5795	4232
final R indices $[I > 2\sigma(I)]$	R1 = 0.066	R1 = 0.049
	R2 = 0.170	R2 = 0.146

$$\phi_s = \frac{\phi_r \eta_s^2 D_s}{\eta_r^2 D_r} \quad (2)$$

where D denotes the area under the emission curve and the subscript designates sample (s) or reference (r), ϕ_s is the corresponding quantum yield, and η is the index of refraction of the appropriate solvent. Bubbling nitrogen through the sample in a septum-capped cell for 25 min sufficed for deoxygenating samples. The method used for extracting lifetimes from emission decay curves has been described previously.[38]

Quenching Studies. A Stern−Volmer plot of the rate constant for decay versus the concentration of chromophore yielded the rate constant for self-quenching and the lifetime at infinite dilution.[39] To characterize buffer-induced quenching, the concentration of porphyrin remained constant, but the buffer concentration varied, at a constant ionic strength. The same kind of analysis provides estimates for the rate constants for quenching by dissolved oxygen via eq 3:

$$k_q = \frac{\frac{\tau_0}{\tau} - 1}{\tau_0[O_2]} \quad (3)$$

where τ_0 is the unquenched lifetime in seconds, τ is the corresponding lifetime in the presence of oxygen, and the concentration of oxygen is 2.55×10^{-4} M at atmospheric pressure. Equation 3 assumes collision-controlled quenching with a second-order rate constant.

Crystallography. For the Pd(*t*D4) structure, the fiber-mounted crystal was a red plate of $C_{32}H_{24}N_6Pd{\cdot}2(C_7H_7O_3S){\cdot}CH_3OH$ having approximate dimensions of 0.38 mm × 0.35 mm × 0.08 mm. The X-rays used were Mo Kα radiation (λ = 0.71073 Å), impacting the crystal at 150(1) K. Programs used for data collection and workup included DENZO/SCALEPACK, XPREP, which determined the space group, and DENZO-SMN.[40] The platform used for the refinement was a LINUX personal computer in conjunction with SHELX-97.[41] Table 1 includes a listing of relevant information regarding data collection and figures of merit for the final refinement. In the case of the Pt(T4) structure, the mounted crystal was a red needle of $C_{44}H_{36}N_8Pt{\cdot}4(H_2O){\cdot}4(NO_3)$ having approximate dimensions of 0.20 mm × 0.08 mm × 0.06 mm. The X-rays used were Cu Kα radiation (λ = 1.54184 Å). The same programs mentioned above facilitated data collection and space group assignment. The programs used for structure solution and refinement were PATTY in DIRDIF99[42] and SHELX-97. The SQUEEZE option in PLATON[43] permitted adjustment of residual electron density. See Table 1 for relevant crystal data.

Instrumentation. The absorption spectrometer was a Varian Cary instrument, while a Varian Cary Eclipse instrument, equipped with a R3896 detector, recorded emission spectra of the porphyrins. The unit used for emission from singlet oxygen was a Horiba Jobin Yvon Fluorolog 3 instrument in conjunction with an indium gallium arsenide detector. The circular dichroic measurements were taken with a JASCO-J180 spectropolarimeter. For the measurement of excited-state lifetimes, the light source was usually a VSL-337-NDS nitrogen dye laser from Laser Science coupled with a DLM-220 dye laser. The detection system included a Hamamatsu R928 phototube, a Pacific Instruments model 277 high-voltage supply, and a Tectronix TDS 520 digitizing oscilloscope. An Optical Building Blocks EasyLife V instrument with a 435 nm LED (light-emitting diode) was the instrument used for lifetimes in the nanosecond range. A Nonius KappaCCD diffractometer was used for the Pd(*t*D4) structure, while a Rigaku Rapid II diffractometer equipped with confocal optics provided data for the solution of the Pt(T4) structure.

RESULTS

Characterization of Porphyrins. Table 2 provides a compilation of absorption and molar absorptivity data for Pt(T4), Pd(T4), and Pd(*t*D4). Like other dicationic porphyrins,[23,34] Pd(*t*D4) is prone to self-association in aqueous solution, as indicated by hypochromism in the Soret region of the absorption spectrum (see the Supporting Information). To avoid this problem, methanol became the solvent of choice for determination of a molar extinction coefficient. A mixed

Table 2. Absorbance Data for Pt(II) and Pd(II) Porphyrins

	Soret		λ_{max} (nm)	
complex	λ_{max} (nm)	ε (mM^{-1} cm^{-1})	Q_1	Q_2
Pt(T4)[31]	402	171	513	545
Pd(T4)[26,47,48]	418	158	525	560
Pd(*t*D4)[a]	407	150	514	550

[a]The solvent is methanol.

dx.doi.org/10.1021/bi401610t | *Biochemistry* 2014, 53, 714−724

solvent containing 50% methanol by volume, which is also capable of dispersing the aggregates, suffices for the control (q = 0) solutions involved in the DNA binding studies described below. The preparation of Pt(T4) was straightforward, but all attempts to prepare isolable amounts of Pt(tD4) in water, benzonitrile, or other organic solvents were unsuccessful. Partial metalation was sometimes evident from absorbance and emission measurements, but dark particulates generally also appeared during heating. Formation of metallic platinum is likely the root complication because the *meso* C−H groups of $H_2$$t$D4 are very susceptible to oxidative attack.[44,45] Formation of Pd(tD4) is less problematic because the kinetics of metal insertion are more favorable for a second-row transition ion, and Pd(II) is also less oxidizing [$E°(Pd^{2+/0})$ = 0.91 V vs $E°(Pt^{2+/0})$ = 1.19 V[46]].

Representations of the molecular structures of Pd(tD4) and Pt(T4) appear in Figures 1 and 2, respectively, complete with atom numbering schemes. In Pd(tD4), the 24 atoms of the porphyrin core are essentially coplanar, but there are systematic deviations from the mean plane. In particular, the meso carbon atoms alternate above and below the mean plane. C2 and C4 both deviate from the plane in the same direction, so the *N*-methylpyridinium-4-yl substituents tend to extend out of the plane. The C_5N plane of each pyridine also rotates out of the plane of the porphyrin. The pyridine connected to C2 twists 53.0° out of the porphyrin plane, and the opposite pyridine twists 56.3° out of plane in the same sense. Presumably because of H···H interactions,[49] each pyridine in turn also induces a slight twisting of the adjacent pyrrole rings. See the Supporting Information for more about atom displacements and packing information. In the other structure, the Pt(T4) molecule sits on a center of inversion, and there are two types of *N*-methylpyridinium-4-yl substituents. The one extending from C10 twists 56.6° away from the mean plane of the porphyrin core, while the other pyridine cants out of the plane in the opposite sense. By way of contrast, the pyridine connected to C5 is more nearly perpendicular to the porphyrin core, and the adjacent pyrrole rings show little tendency to twist out of plane as a consequence. However, there is a 50:50 disorder associated with the dihedral angle subtended by the pyridine, which is either +79.9° or −79.9°. The disorder also affects the positions of half of the nitrate anions.

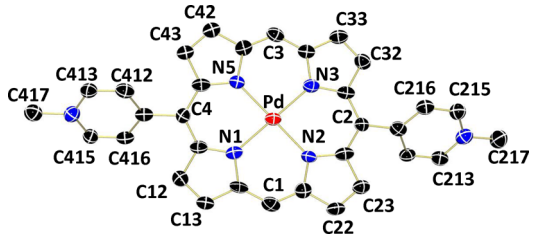

Figure 1. Representation of the cation in [Pd(tD4)]$(PTS)_2$·CH_3OH with thermal ellipsoids set at 50% probability. Hydrogen atoms have been omitted for the sake of clarity.

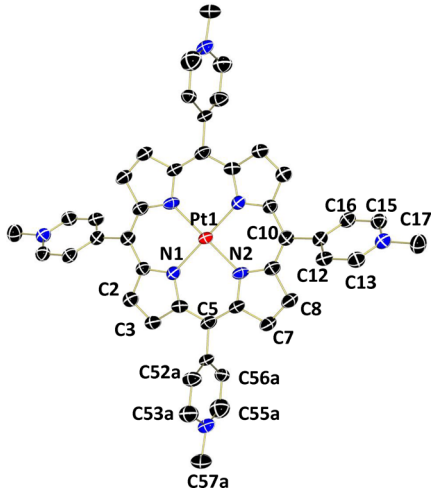

Figure 2. Representation of the cation in [Pt(T4)]$(NO_3)_4$·$4(H_2O)$ with thermal ellipsoids set at 50% probability. Hydrogen atoms have been omitted for the sake of clarity.

Photophysics. In general, the excited-state lifetimes of the palladium(II) porphyrins are dependent on concentration and medium. For the triplet state of Pd(T4), Harriman and co-workers reported a lifetime of 115 μs in pure water under a nitrogen atmosphere but provided no information about concentration.[26] In this study at a working porphyrin concentration of 2.5 μM, the measured lifetime of Pd(T4) is 175 μs in a deaerated Tris nitrate buffer (pH 7.5), containing 0.01 M Tris nitrate and 0.04 M sodium nitrate. On the other hand, at a Pt(T4) concentration of 2.8 μM and a chloride concentration of 0.025 M, the lifetime is only 65 μs. Chloride evidently acts as a quencher and/or catalyzes self-quenching of the porphyrin. Indeed, in deaerated water and in the absence of an added electrolyte, the lifetime of the chloride salt of Pd(T4) extrapolates to 209 μs (τ_0) at infinite dilution, and the plot yields an apparent self-quenching constant of 3.3×10^8 M^{-1} s^{-1}. Tris amine acts as a quencher, but the rate constant (k_q) is small at 1.8×10^5 M^{-1} s^{-1}. The Pd(tD4) ion also exhibits self-quenching with a rate constant of 1.8×10^8 M^{-1} s^{-1} in 50% methanol with tosylate as the counterion. At an infinite dilution of porphyrin in the absence of oxygen, the lifetime extrapolates to 311 μs. Unless excess tosylate is present in solution, the anion is effectively nonquenching because the quenching constant is only 6.5×10^6 M^{-1} s^{-1}. Experimentally measured emission quantum yields (ϕ's) obtained in the Tris nitrate and

Table 3. Photophysical Data, Including Triplet Lifetimes

chromophore	τ_0 (μs)[a]	τ (μs)	ϕ[b]	k_q (M^{-1} s^{-1})	$\theta_q(O_2)$[c]
Pd(T4)	209	1.6	0.016	2.5×10^9	0.99
Pd(T4)·TT[t_4]	218	15	0.0057	2.5×10^8	0.93
Pd(T4)·CG[ga_3]	204	32	0.011	1.1×10^8	0.84
H_2T4·[poly(dA-dT)]$_2^{50}$	1600	20		2.0×10^8	0.99
H_2T4·[poly(dG-dC)]$_2^{50}$	1300	30		1.3×10^8	0.98
Pd(tD4)·TT[t_4]	650	27	0.016	1.4×10^8	0.96
Pd(tD4)·CG[ga_3]	625	33	0.029	1.1×10^8	0.95

[a]Under nitrogen, corrected for self-quenching as appropriate. [b]Emission yield. [c]Fractional efficiency of quenching by O_2 (see the text).

Table 4. Physical Data Pertaining to DNA-Bound Porphyrins

		absorption		CD	
	DNA host	$\Delta\lambda$ (nm)	% H	λ (nm)	$\Delta\varepsilon$ (M^{-1} cm^{-1})
		Bulky Porphyrins			
Pd(T4)	CG[ga_3]	19	33	435	−33
	TT[t_4]	8	14	411−435	+8 to −4
Pd(T4)[48]	[poly(dG-dC)]$_2$	20	35	436	−24
	[poly(dA-dT)]$_2$	8	8	417−440	+9 to −6
Cu(T4)[23,27]	CG[ga_3]	14	45	434	−25
	TT[t_4]	5	2	420	+15
		Sterically Friendly Porphyrins			
Pd(*t*D4)	CG[ga_3]	19	48	424	−14
	TT[t_4]	17	28	417	−14
Cu(*t*D4)[23]	CG[t_4]	16	28	414	−10
	TT[t_4]	16	24	415	−20
Cu(*t*Me$_2$D4)[34]	[poly(dG-dC)]$_2$	23	52	442	−20
	[poly(dA-dT)]$_2$	16	32	434	−18

sodium nitrate buffer are listed in Table 3. See Figure S2 of the Supporting Information to appreciate the influence of the detector gate setting on the measurement.

DNA Binding Studies. Uptake of Pd(T4) by an excess of the G≡C rich CG[ga_3] host induces spectral changes that are completely consistent with intercalative binding; however, the same porphyrin binds externally to TT[t_4]. Thus, interaction with CG[ga_3] induces a large bathochromic shift of the Soret band, along with a 33% hypochromic response, and a negative induced circular dichroic (iCD) signal, reaching a maximum at almost the same wavelength (Table 4). Data listed in Table 4 reveal that the induced spectral changes are practically identical to those reported by Barnes et al., who investigated intercalation into [poly(dG-dC)]$_2$.[48] In contrast, the $\Delta\lambda$ and H values induced by binding Pd(T4) to TT[t_4] decrease by more than half, in keeping with results obtained with the analogous Cu(T4) derivative and the same hairpin hosts (Table 4). The spectral changes and the absence of any significant emission intensity from the bound form of Cu(T4) are strong indications of external binding and ready access of the copper(II) center.[34,51] The other classic sign of external binding is the positive iCD signal reported for the adduct of Cu(T4) with TT[t_4]. The iCD signal for the corresponding adduct of Pd(T4) exhibits a relatively strong positive branch but is clearly bisignate. See Figure 3 for an overlay of the iCD signals obtained in the presence of excess host. Barnes et al. obtained similar results when they studied the uptake of Pd(T4) by excess [poly(dA-dT)]$_2$.[48] They attempted to model the results theoretically and concluded the ligand binds externally in the major groove, with the plane of the porphyrin tilted with respect to the axis of the DNA double helix.

In contrast to the results described above, uptake of the sterically friendly porphyrin Pd(*t*D4) induces large $\Delta\lambda$ and H responses, independent of the base composition of the DNA host. The iCD signals are also uniformly negative. All findings are strictly consistent with intercalation.

In each titration, uptake is facile, and a base pair:porphyrin ratio (q) of 16:1 is generally sufficiently high to approach the limiting spectrum. Absorbance changes that occur with titration of CG[ga_3] into a solution of Pd(*t*D4) are typical and appear in Figure 4. The same figure also shows that binding to CG[ga_3] shifts the maximum of the singlet emission from 562 to 579 nm, while that of the triplet emission shifts from around 700 to 718 nm. Finally, the data reveal how intercalation into a DNA host inhibits the quenching by dissolved oxygen. Thus, the intensity of the triplet emission, which is almost nil in the absence of DNA, markedly increases when the porphyrin binds

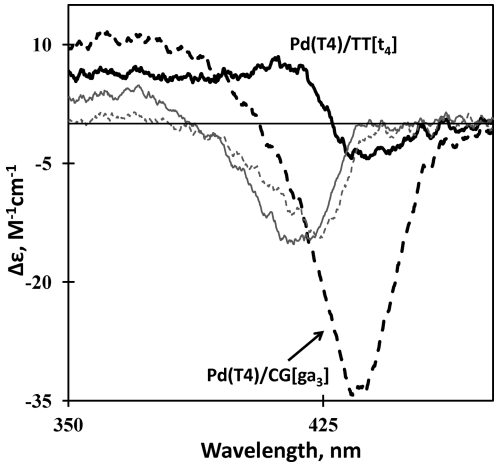

Figure 3. Induced CD spectra of Pd(T4) bound to DNA hairpins TT[t_4] (thick solid line) and CG[ga_3] (thick dashed line) and of Pd(*t*D4) bound to TT[t_4] (thin solid line) and CG[ga_3] (thin dashed line). All are limiting spectra obtained at q = 32, where q is the base pair:porphyrin ratio.

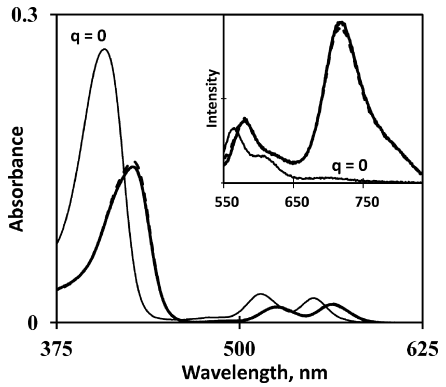

Figure 4. Absorption spectra of 2.0 μM Pd(*t*D4) at q = 0 (thin solid line) and in the presence of the DNA hairpin CG[ga_3] at q = 16 (dashed line) and q = 32 (thick solid line). The inset shows the corresponding emission spectra measured at q = 0 (thin solid line), q = 16 (dashed line), and q = 32 (thick solid line).

dx.doi.org/10.1021/bi401610t | *Biochemistry* 2014, 53, 714−724

to CG[ga$_3$]. Note that, in contrast, diffusional quenching by oxygen has comparatively little effect on the higher-energy signal, because of lifetime considerations.

Quenching by O_2. Table 3 includes a summary of oxygen-induced quenching results. They reveal that external binding to DNA significantly reduces access by molecular oxygen, as the rate constant for lifetime quenching decreases by an order of magnitude for the bound form. Intercalation into DNA proves to be more effective than external binding, but the quenching rate constants differ by a factor of only 2. In the end, the fractional efficiency of quenching by molecular oxygen [$\theta_q(O_2) = \tau k_q[O_2]$] is just 10% lower for intercalated relative to externally bound Pd(T4). Even though intercalated Pd(*t*D4) extends only half as many pyridinium-4-yl substituents away from the surface of the CG[ga$_3$] host, the calculated quenching constant k_q is essentially identical to that obtained with Pd(T4). On the other hand, the k_q value is ~25% larger when Pd(*t*D4) intercalates into the more flexible TT[t$_4$] host. One of the most striking observations is that for intercalated Pd(*t*D4) the fractional efficiency of oxygen-induced quenching approaches unity, irrespective of the host. This result is a reflection of the intrinsically long lifetime of the bound form of Pd(*t*D4).

In a D_2O-based medium, consistent with the $\theta_q(O_2)$ results, Figure 5 shows that the emission signal obtained from singlet oxygen is only ~10% weaker when the Pd(T4) sensitizer intercalates into the CG[ga$_3$] host, compared with that for external binding to TT[t$_4$]. The singlet oxygen emission signal also turns out to be ~2-fold stronger when Pd(*t*D4) serves as the sensitizer, regardless of whether it intercalates into CG[ga$_3$] or TT[t$_4$] (Figure 5). Finally, the same figure shows that the free ligands are superior emission sensitizers, although a change in the solubility of oxygen could bias the results for free Pd(*t*D4). The medium is unique in that case in that it contains 50% d_4-MeOH.

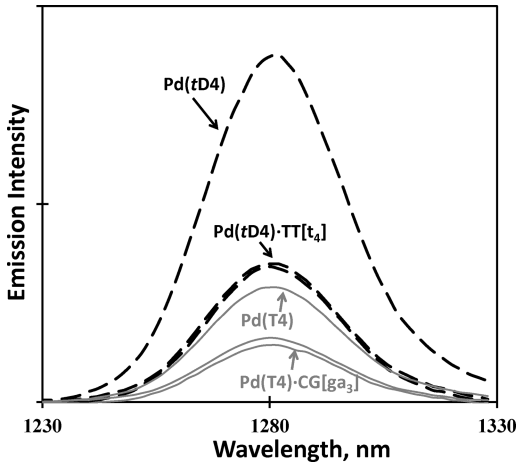

Figure 5. Singlet oxygen emission spectra sensitized by Pd(T4) (thin gray line) or Pd(*t*D4) (dashed line). Pd(*t*D4) always produces a stronger signal, and free porphyrins yield stronger signals than bound forms. Finally, for either porphyrin, binding to TT[t$_4$] or CG[ga$_3$] results in a similar sensitized emission signal.

DISCUSSION

Cationic porphyrins generally adopt one of three well-recognized motifs for binding to standard B-form DNA. One is intercalation, first reported by Fiel and co-workers.[16] The others are external (or groove) binding and, under some conditions, outside stacking (or aggregation) along the surface of the DNA host.[4,15,52] Because the shape of a porphyrin is not complementary to that of B-form DNA, high-affinity binding always involves a structural reorganization of the host, i.e., an induced fit.[17] External binding, the norm for metalloporphyrins bearing axial ligands,[3,4] involves local melting of the DNA structure and formation of a binding pocket to optimize a mix of hydrophobic and electrostatic interactions. On the other hand, metalated forms that lack ligands, e.g., Cu(T4) and Pd(T4), are also capable of intercalating. The structural reorganization required for intercalative binding entails duplex unwinding but generally preserves the double-helical structure.[53] *A priori*, intercalation might appear to be the ideal binding motif for porphyrins like H_2T4, given the relatively flat aromatic interior as well as cationic substituent groups that extend off the periphery. However, a structural study reveals that *N*-methylpyridinium-4-yl substituents sterically clash with sugar−phosphate residues that line the walls of the host's minor groove.[20] The upshot is that intercalation is only feasible amidst G≡C rich base sequences, where the energetic cost of partial melting lowers the affinity for external binding.[17] More recent work reveals that sterically friendly tri- and disubstituted porphyrins behave differently and act as universal intercalators.[21,22,24,34,54] Thus, Cu(*t*D4) binds by interaction into B-form DNA regardless of the base sequence. Those developments led to this investigation of whether intercalative binding is compatible with the sensitization of singlet oxygen.

DNA Binding Motifs and Oxygen Accessibility. The Pd(T4) system allows a comparison of oxygen-induced quenching efficiencies for intercalated versus externally bound forms, the two binding motifs most compatible with a long-lived excited state. More specifically, absorbance and iCD results reveal that bulky Pd(T4) intercalates into the CG[ga$_3$] host but binds externally to the more flexible TT[t$_4$] host (*vide supra*). The iCD signal obtained when Pd(T4) binds to TT[t$_4$] is nonstandard, but the iCD signal is also bisignate when Pd(T4) or Ni(T4) binds externally to [poly(dA-dT)]$_2$.[18,48] Barnes used exciton coupling theory to rationalize the result obtained with [poly(dA-dT)]$_2$;[48] however, geometry is an issue because the host is likely to depart from canonical B-form structure, at least in the vicinity of the ligand, in achieving an induced fit. As some degree of ligand restructuring is also possible, a chiral distortion within the ligand framework itself could also help shape the iCD signal. Indeed, the literature reveals that porphyrins are capable of a variety of distortions.[55] The nature and extent of the distortion may depend upon the metal present, and that may account for the fact that the adduct obtained with Cu(T4) and TT[t$_4$] exhibits a strictly positive iCD signal. Any such distortion in the Pd(T4) framework has little effect on the intrinsic excited-state lifetime (τ_0), as revealed by data in Table 3. On the other hand, intercalation and external binding with DNA both strongly inhibit quenching by molecular oxygen. The fact that external binding to DNA is so effective at screening the porphyrin from dissolved oxygen is consistent with the idea of an intimate, well-sculpted binding pocket.

The notion of an induced fit and a well-conformed binding pocket seems compelling in the context of understanding tight binding of porphyrins to ds DNA.[17] Structural confirmation is, however, lacking. A crystal structure is available, but it may not relate because the porphyrin in it lodges between adjacent DNA hosts,[56] in contrast to what one expects to find in solution. In this light, it is time to make mention of an earlier

study, which reportedly detailed the first measurement of emission from dioxygen sensitized by H_2T4 bound to DNA and presented evidence of slow oxygen-induced quenching of externally bound porphyrin.[57] On the basis of their time-resolved studies of triplet absorption, Kruk et al. concluded that H_2T4 adopts two external binding motifs with $[poly(dA\text{-}dT)]_2$, because of the biphasic decay observed. They went on to conclude that one of the motifs exhibits much slower quenching than the other. Invoking the canonical structure of B-form DNA, the authors further proposed that the ligand subject to slow quenching lodges edge-on in the minor groove of the DNA host, while the more exposed form adopts a face-on binding motif.

In contradistinction, Pd(*t*D4) intercalates into both TT[t_4] and CG[ga_3]. Here the iCD signals are consistently negative, perhaps because intercalation is at once less conducive to variations in ligand structure and more supportive of strong exciton coupling with DNA bases. Intercalation into DNA also induces a large increase in the τ_0 of the Pd(*t*D4) system. Kelly and co-workers have found that the lifetime of Pt(T4) also increases somewhat with binding to mononucleotides, and they attribute this effect to the enhanced rigidity of the bound form.[69] In that context, the large impact binding has on the τ_0 of Pd(*t*D4) would be even more impressive, because there are fewer substituents to constrain. The sheer number of exposed substituent arms also has little impact on oxygen-induced quenching, because the rate constants obtained for Pd(*t*D4) are almost the same as that of intercalated Pd(T4). On the other hand, flexibility within the host may promote oxygen-induced quenching, because the rate constant is ∼25% greater for the adduct with TT[t_4], as opposed to the more rigid CG[ga_3] hairpin (Table 3). The efficiency of oxygen-induced quenching nevertheless approaches 95% for both adducts because of the exceptionally long excited-state lifetimes.

Sensitization of Singlet Oxygen. Singlet oxygen is a product of quenching in all cases (Figure 5). Note, however, that the emission intensity does not reflect the relative quantum yield of singlet oxygen production. Rather, the emission intensity depends on the steady-state concentration of singlet oxygen that results from a series of competing kinetic processes. Along the lines developed by Verlhac and co-workers,[58] one can show that the emission intensity is proportional to eq 4:

$$\frac{\theta_{isc}\tau_d}{\tau_a} \times \frac{I_0}{\frac{1}{\tau_0} + \frac{1}{\tau_a}} \qquad (4)$$

where I_0 is the rate of photon absorption and θ_{isc} is the intersystem crossing efficiency to the triplet state of the porphyrin. $\tau_a = (k_q[O_2])^{-1}$ and $\tau_d = k_d^{-1}$ are the time constants for the appearance and decay, respectively, of singlet oxygen in solution. (Note that eq 4 assumes a steady-state concentration of the porphyrin excited state is also present in solution.) The variation in the τ_d/τ_a ratio undoubtedly explains why free porphyrin always produces a more intense singlet oxygen signal than a bound form, even when the net oxygen-induced quenching efficiencies are similar. The steady-state concentration of singlet oxygen is lower for bound forms because DNA selectively increases the time constant for the appearance of singlet oxygen by impeding the access of O_2 to the excited porphyrin. From that point of view, one pair of comparisons really stands out. More specifically, Figure 5 reveals that the bound forms of Pd(tD4) produce higher singlet oxygen intensities than free Pd(T4). This result is striking because Pd(T4) is capable of yielding one of the highest steady-state levels of singlet oxygen, because of a relatively short τ_a and the fact that the phosphorescence quenching is virtually complete (θ_q = 0.99). On what may be a related note, Verlhac and co-workers have reported that Pd(T4) is anomalous in being ∼6 times less efficient than its parent, H_2T4, at sensitizing singlet oxygen.[58] On the other hand, Harriman and co-workers report the yield is as high as 80%.[26]

Yet another possibility to consider is that the steady-state concentration of *P may differ for Pt(T4) and Pt(*t*D4). Any variation in the intersystem crossing efficiency θ_{isc} is, however, likely to be small. The literature value is typically around 0.9 with or without metal present in the cationic porphyrin.[59,60] In addition, the intersystem crossing efficiency also approaches unity in Pd(TPP), the tetraphenyl analogue of Pd(T4).[61] For bound forms of Pd(T4), reductive quenching of the singlet precursor could, nevertheless, suppress triplet (*P) formation. The transfer of an electron from guanine to the singlet excited state can, indeed, be useful for photodynamic therapy by a type I mechanism that is independent of oxygen.[50] The latter effect may have some role, but the fact remains that Figure 5 reveals that even the unbound form of Pd(T4) generates a low intensity of emission from $^*O_2$ by comparison with that of Pd(*t*D4).

Oxygen-Induced Quenching Mechanisms. The contrasting behavior of Pd(T4) and Pd(*t*D4) may instead reflect a disparity in quenching mechanisms, as there are a number of possibilities. More specifically, Scheme 2 presents a very simplified outline of a process including three distinct and well-recognized O_2-induced quenching mechanisms.[62−64] In the scheme, P and *P symbolize a porphyrin in its ground state and triplet excited state, respectively, and C represents an intermediate complex of the form $^*[P^{\delta+}\cdots O_2^{\delta-}]$. $^2P^+$ denotes an oxidized form, while O_2 and $^*O_2$ are respective designations for the ground state and first excited state, respectively, of the dioxygen molecule. Finally, k_{el} denotes the rate constant for electron-transfer quenching, while k_{en} and k_{ic} designate rate constants for energy transfer and internal conversion back to the ground state via complex C, respectively. In this view, the steady-state concentration of $^*O_2$ depends on the product of two efficiency factors, θ_{isc} and θ_{en}, where the efficiency of energy transfer quenching $\theta_{en} = k_{en}/(k_{en} + k_{el} + k_{ic})$. All three of the envisioned quenching pathways in Scheme 2 appear to be viable for the reactive excited state of Pd(T4). Calculations suggest formation of the superoxide ion is possible by photoinduced electron transfer, but the favorable driving force of $\Delta G_{el} \approx -0.06$ eV is very modest. The latter estimate assumes a reduction potential of 1.41 V for the $^2P^+/P$ couple and a calculated triplet energy of 1.80 eV.[26] The driving force for energy transfer turns out to be much greater ($\Delta G_{en} \approx -0.82$

Scheme 2

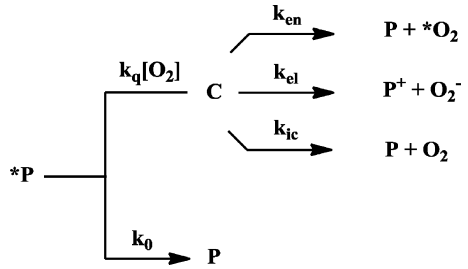

dx.doi.org/10.1021/bi401610t | *Biochemistry* 2014, 53, 714−724

eV). However, the transmission coefficient is probably low because encapsulaton of the donor by the DNA host compromises the orbital overlap required for the transfer of energy to O_2. (Through-space energy transfer is impractical because the transitions involved each represent spin-forbidden transitions carrying virtually zero oscillator strength.[65]) In the k_{ic} pathway, the paramagnetic dioxygen molecule effectively catalyzes the radiationless decay process while releasing 1.80 eV worth of excitation energy into vibrational degrees of freedom.[62] Formation of charge-transfer complex C enhances coupling to the spin system of the quencher and prolongs the interaction so that vibronic relaxation has time to occur. Variation in θ_{en} explains the data in Figure 5, if for Pd(*t*D4) the k_{en} pathway for oxygen-induced triplet quenching is more efficient by comparison than the k_{ic} and/or k_{el} pathway than is the case with Pd(T4). Perhaps comparatively easy access to the unsubstituted C10 and C20 atoms of Pd(*t*D4) accounts for the improved orbital overlap with the quencher and an enhanced rate of energy transfer.

CONCLUSIONS

Studies with bulky Pd(T4) reveal that O_2-induced quenching of the triplet excited state is only slightly less efficient when the porphyrin intercalates as opposed to binding externally to ds DNA. Also, energy-transfer quenching is a strikingly more efficient process with the sterically friendly analogue, Pd(*t*D4), which exclusively binds by intercalation. Better orbital overlap in the precursor complex may account for the enhanced energy-transfer rate, because of the ready access to the C10 and C20 *meso* atoms of Pd(*t*D4). Bulky substituents on the periphery of the porphyrin may therefore impact the sensitization of singlet oxygen as well as the binding motif. Pd(T4) and Pd(*t*D4) both act as sensitizers, but the emission intensity from singlet O_2 does not necessarily reflect the relative yield. The confounding effect is that the time constant for formation of singlet O_2 can exceed that of the decay when binding to DNA restricts access to the porphryin. As a consequence, the sensitized emission signal is invariably weaker when DNA is present, even though the quenching efficiency approaches 100% for bound Pd(*t*D4), because of an impressively long triplet lifetime. It is clear that achieving a full understanding of how host and guest structure influence DNA binding will require a great deal more work. Induced changes in conformation(s) affect iCD signals, binding constants, and chemical as well as biological activity, while structural fluctuations potentially influence reaction rates. Taking advantage of opportunities available, many groups have begun exploiting conformational changes in the course of developing molecular machines and sensing strategies.[66−68]

ASSOCIATED CONTENT

Supporting Information

Experimental details and figures showing the influence solvent composition has on the absorption of Pd(*t*D4) as well as the effect the mode of data collection has on emission spectra and other figures showing deviations of core atoms from the mean plane of Pd(*t*D4) and packing within its lattice as well as deviations of core atoms from the mean plane of Pt(T4). This material is available free of charge via the Internet at http://pubs.acs.org.

AUTHOR INFORMATION

Corresponding Author

*Department of Chemistry, Purdue University, 560 Oval Dr., West Lafayette, IN 47907. E-mail: mcmillin@purdue.edu. Phone: (765) 494-5452. Fax: (765) 494-0239.

Funding

The National Science Foundation funded this research via Grants CHE 0847229 and CBET-11097833.

Notes

The authors declare no competing financial interests.

ABBREVIATIONS

H_2T4, 5,10,15,20-tetra(*N*-methylpyridinium-4-yl)porphyrin; Pd(T4), [5,10,15,20-tetra(*N*-methylpyridinium-4-yl)-porphyrinato]palladium(II); H_2*t*D4, 5,15-di(*N*-methylpyridinium-4-yl)porphyrin; Pd(*t*D4), [*trans*-5,15-di(*N*-methylpyridinium-4-yl)porphyrinato]palladium(II); H_2TMAP, 5,10,15,20-tetra(*N*,*N*,*N*-trimethylanilinium-4-yl)porphyrin; CD, circular dichroism; MeCN, acetonitrile; TLC, thin-layer chromatography; PTS, *p*-toluene sulfonate; TT[t_4], 5′-GATTACttttGTAATC-3′; CG[ga_3], 5′-GACGACgaaaGTCGTC-3′; dpm, dipyrromethane; Pd(DMSO)$_2$Cl$_2$, bis(dimethyl sulfoxide)-bis(chloro)palladium(II); $[Ru(bpy)_3]^{2+}$, tris(2,2′-bipyridinyl)-ruthenium(II); θ, efficiency factor; ϕ, quantum yield; τ, lifetime or time constant; k_q, quenching rate constant; $\Delta\lambda$, wavelength shift; % *H*, percent hypochromism; *P, triplet state of porphyrin; DMF, *N*,*N*-dimethylformamide; DCM, dichloromethane; HNO_3, nitric acid; TBAN, tetrabutylammonium nitrate; KPF_6, potassium hexafluorophosphate; ds, double-stranded; d_4-MeOH, fully deuterated methanol; *q*, ratio of DNA base pairs to porphyrin concentration; ΔG_{el}, free energy of electron transfer; ΔG_{en}, free energy of energy transfer.

REFERENCES

(1) Fiel, R. J., Howard, J. C., Mark, E. H., and Dattagupta, N. (1979) Interaction of DNA with a porphyrin ligand-evidence for intercalation. *Nucleic Acids Res. 6*, 3093−3118.

(2) Fiel, R. J. (1989) Porphyrin−nucleic-acid interactions: A review. *J. Biomol. Struct. Dyn. 6*, 1259−1275.

(3) Pasternack, R. F., and Gibbs, E. J. (1996) Porphyrin and metalloporphyrin interactions with nucleic acids. *Met. Ions Biol. Syst. 33*, 367−397.

(4) McMillin, D. R., and McNett, K. M. (1998) Photoprocesses of copper complexes that bind to DNA. *Chem. Rev. 98*, 1201−1219.

(5) Fiel, R. J., Dattagupta, N., Mark, E. H., and Howard, J. C. (1981) Induction of DNA damage by porphyrin photosensitizers. *Cancer Res. 41*, 3543−3545.

(6) Henderson, B. W., and Dougherty, T. J. (1992) How does photodynamic therapy work. *Photochem. Photobiol. 55*, 145−157.

(7) Bonnett, R. (2000) *Chemical aspects of photodynamic therapy*, Gordon and Breach, Singapore.

(8) Croke, D. T., Perrouault, L., Sari, M. A., Battioni, J. P., Mansuy, D., Helene, C., and Ledoan, T. (1993) Structure-activity relationships for DNA photocleavage by cationic porphyrins. *J. Photochem. Photobiol., B 18*, 41−50.

(9) Hamblin, M. R., O'Donnell, D. A., Murthy, N., Contag, C. H., and Hasan, T. (2002) Rapid control of wound infections by targeted photodynamic therapy monitored by in vivo bioluminescence imaging. *Photochem. Photobiol. 75*, 51−57.

(10) Kasturi, C., and Platz, M. S. (1992) Inactivation of lambda-phage with 658 nm light using a DNA-binding porphyrin sensitizer. *Photochem. Photobiol. 56*, 427−429.

(11) Han, F. X. G., Wheelhouse, R. T., and Hurley, L. H. (1999) Interactions of TMPyP4 and TMPyP2 with quadruplex DNA.

Structural basis for the differential effects on telomerase inhibition. *J. Am. Chem. Soc. 121*, 3561−3570.
(12) Parkinson, G. N., Ghosh, R., and Neidle, S. (2007) Structural basis for binding of porphyrin to human telomeres. *Biochemistry 46*, 2390−2397.
(13) Nicoludis, J. M., Miller, S. T., Jeffrey, P. D., Barrett, S. P., Rablen, P. R., Lawton, T. J., and Yatsunyk, L. A. (2012) Optimized end-stacking provides specificity of N-methyl mesoporphyrin IX for human telomeric G-quadruplex DNA. *J. Am. Chem. Soc. 134*, 20446−20456.
(14) Carvlin, M. J., and Fiel, R. J. (1983) Intercalative and nonintercalative binding of large cationic porphyrin ligands to calf thymus DNA. *Nucleic Acids Res. 11*, 6121−6139.
(15) Manono, J., Marzilli, P. A., Fronczek, F. R., and Marzilli, L. G. (2009) New porphyrins bearing pyridyl peripheral groups linked by secondary or tertiary sulfonamide groups: Synthesis and structural characterization. *Inorg. Chem. 48*, 5626−5635.
(16) Fiel, R. J., and Munson, B. R. (1980) Binding of meso-tetra(4-N-methylpyridyl) porphine to DNA. *Nucleic Acids Res. 8*, 2835−2842.
(17) McMillin, D. R., Shelton, A. H., Bejune, S. A., Fanwick, P. E., and Wall, R. K. (2005) Understanding binding interactions of cationic porphyrins with B-form DNA. *Coord. Chem. Rev. 249*, 1451−1459.
(18) Pasternack, R. F., Gibbs, E. J., and Villafranca, J. J. (1983) Interactions of porphyrins with nucleic-acids. *Biochemistry 22*, 2406−2414.
(19) Marzilli, L. G. (1990) Medical aspects of DNA-porphyrin interactions. *New J. Chem. 14*, 409−420.
(20) Lipscomb, L. A., Zhou, F. X., Presnell, S. R., Woo, R. J., Peek, M. E., Plaskon, R. R., and Williams, L. D. (1996) Structure of a DNA-porphyrin complex. *Biochemistry 35*, 2818−2823.
(21) Wall, R. K., Shelton, A. H., Bonaccorsi, L. C., Bejune, S. A., Dube, D., and McMillin, D. R. (2001) H_2D3: A cationic porphyrin designed to intercalate into B-form DNA (H_2D3 = trans-di(N-methylpyridium-3-yl)porphyrin). *J. Am. Chem. Soc. 123*, 11480−11481.
(22) Bejune, S. A., Shelton, A. H., and McMillin, D. R. (2003) New dicationic porphyrin ligands suited for intercalation into B-form DNA. *Inorg. Chem. 42*, 8465−8475.
(23) Briggs, B. N., Gaier, A. J., Fanwick, P. E., Dogutan, D. K., and McMillin, D. R. (2012) Cationic copper(II) porphyrins intercalate into domains of double-stranded RNA. *Biochemistry 51*, 7496−7505.
(24) Wu, S., Li, Z., Ren, L. G., Chen, B., Liang, F., Zhou, X., Jia, T., and Cao, X. P. (2006) Dicationic pyridium porphyrins appending different peripheral substituents: Synthesis and studies for their interactions with DNA. *Bioorg. Med. Chem. 14*, 2956−2965.
(25) Yamamoto, T., Tjahjono, D. H., Yoshioka, N., and Inoue, H. (2003) Interaction of dicationic bis(imidazoliumyl)porphyrinatometals with DNA. *Bull. Chem. Soc. Jpn. 76*, 1947−1955.
(26) Brun, A. M., and Harriman, A. (1994) Enery-transfer and electron-transfer processes involving palladium porphyrins bound to DNA. *J. Am. Chem. Soc. 116*, 10383−10393.
(27) Lugo-Ponce, P., and McMillin, D. R. (2000) DNA-binding studies of Cu(T4), a bulky cationic porphyrin. *Coord. Chem. Rev. 208*, 169−191.
(28) Laha, J. K., Dhanalekshmi, S., Taniguchi, M., Ambroise, A., and Lindsey, J. S. (2003) A scalable synthesis of meso-substituted dipyrromethanes. *Org. Process Res. Dev. 7*, 799−812.
(29) Cotton, F. A., and Francis, R. (1960) Sulfoxides as ligands. 1. A preliminary survey of methyl sulfoxide complexes. *J. Am. Chem. Soc. 82*, 2986−2991.
(30) Cotton, F. A., Francis, R., and Horrocks, W. D. (1960) Sulfoxides as ligands. 2. The infrared spectra of some dimethyl sulfoxide complexes. *J. Phys. Chem. 64*, 1534−1536.
(31) Pasternack, R. F., Brigandi, R. A., Abrams, M. J., Williams, A. P., and Gibbs, E. J. (1990) Interactions of porphyrins and metalloporphyrins with single-stranded poly(dA). *Inorg. Chem. 29*, 4483−4486.
(32) Batinic-Haberle, I., Spasojevic, I., Hambright, P., Benov, L., Crumbliss, A. L., and Fridovich, I. (1999) Relationship among redox potentials, proton dissociation constants of pyrrolic nitrogens, and in vivo and in vitro superoxide dismutating activities of manganese(III) and iron(III) water-soluble porphyrins. *Inorg. Chem. 38*, 4011−4022.
(33) Sambrook, J., Fritsch, E. F., and Maniatis, T. (1989) *Molecular cloning: A laboratory manual*, 2nd ed., Vol. 3, Cold Spring Harbor Laboratory Press, Plainview, NY.
(34) Shelton, A. H., Rodger, A., and McMillin, D. R. (2007) DNA binding studies of a new dicationic porphyrin. Insights into interligand interactions. *Biochemistry 46*, 9143−9154.
(35) Demas, J. N., and Crosby, G. A. (1971) Measurement of photoluminescence quantum yields-review. *J. Phys. Chem. 75*, 991−1024.
(36) Parker, C. A., and Rees, W. T. (1960) Correction of fluorescence spectra and measurement of fluorescence quantum efficiency. *Analyst (Cambridge, U.K.) 85*, 587−600.
(37) Caspar, J. V., and Meyer, T. J. (1983) Photochemistry of $Ru(bpy)_3^{2+}$: Solvent effects. *J. Am. Chem. Soc. 105*, 5583−5590.
(38) Liu, F., Cunningham, K. L., Uphues, W., Fink, G. W., Schmolt, J., and McMillin, D. R. (1995) Luminescence quenching of copper(II) porphyrins with Lewis-bases. *Inorg. Chem. 34*, 2015−2018.
(39) Turro, N. (1978) *Modern molecular photochemistry*, pp 247−248, Benjamin/Cumminngs, Menlo Park, CA.
(40) Otwinowski, Z., and Minor, W. (1997) Processing of X-ray diffraction data collected in oscillation mode. *Methods Enzymol. 276*, 307−326.
(41) Sheldrick, G. M. (2008) A short history of SHELX. *Acta Crystallogr. A64*, 112−122.
(42) Beurskens, P. T., Beurskens, G., deGelder, R., Garcia-Granda, S., Gould, R. O., and Smits, J. M. M. (2008) *The DIRDIF2008 Program System*, Crystallography Laboratory, University of Nijmegen, Nijmegen, The Netherlands.
(43) Spek, A. L. (1997) *PLATON. Molecular graphics program*, University of Utrecht, Utrecht, The Netherlands.
(44) Dogutan, D. K., and Lindsey, J. S. (2008) Investigation of the scope of a new route to ABCD-bilanes and ABCD-porphyrins. *J. Org. Chem. 73*, 6728−6742.
(45) Furhop, J.-H. (1978) Irreversibe reactions on porphyrin periphery. In *The Porphyrins, Structure and Synthesis, Part B* (Dolphin, D., Ed.) pp 131−159, Academic Press, New York.
(46) Colom, F. (1985) Nickel, palladium, and platinum. In *Standard Potentials in Aqueous Solution* (Bard, A. J., Parsons, R., and Jordan, J., Eds.) Marcel Dekker, Inc., New York.
(47) Strickland, J. A., Banville, D. L., Wilson, W. D., and Marzilli, L. G. (1987) Metalloporphyrin effects on properties of DNA polymers. *Inorg. Chem. 26*, 3398−3406.
(48) Barnes, N. R., Stroud, P. D., Robinson, K. E., Horton, C., and Schreiner, A. F. (1999) 5,10,15,20-Tetrakis(4-N-methylpyridyl)-porphyrinato-palladium(II) as a differentiation probe for sensing binding modes with B-DNA duplexes: Electronic MCD and CD spectra. *Biospectroscopy 5*, 179−188.
(49) Fleischer, E. B., Webb, L. E., and Miller, C. K. (1964) Crystal molecular structures of some metal tetraphenylporphines. *J. Am. Chem. Soc. 86*, 2342−2347.
(50) Chirvony, V. S., Galievsky, V. A., Kruk, N. N., Dzhagarov, B. M., and Turpin, P. Y. (1997) Photophysics of cationic 5,10,15,20-tetrakis-(4-N-methylpyridyl)porphyrin bound to DNA, poly(dA-dT)$_2$ and poly(dG-dC)$_2$: On a possible charge transfer process between guanine and porphyrin in its excited singlet state. *J. Photochem. Photobiol., B 40*, 154−162.
(51) Hudson, B. P., Sou, J., Berger, D. J., and McMillin, D. R. (1992) Luminescence studies of the intercalaton of Cu(TMPyP4) into DNA. *J. Am. Chem. Soc. 114*, 8997−9002.
(52) Armitage, B. A. (2006) DNA-templated assembly of helical multichromophore aggregates. In *Molecular and Supramolecular Photochemistry* (Ramamurthy, V., and Schanze, K. S., Eds.) pp 255−287, CRC Press, Boca Raton, FL.
(53) Calladine, C. R., and Drew, H. R. (1997) *Understanding DNA*, Academic Press, New York.
(54) Andrews, K., and McMillin, D. R. (2008) A pared-down version of 5,10,15,20-tetra(N-methylpyridinium-4-yl)porphyrin intercalates

into B-form DNA regardless of base composition: Binding studies of tri(N-methylpyridinium-4-yl)porphyrins. *Biochemistry 47*, 1117−1125.
(55) Shelnutt, J. A., Song, X. Z., Ma, J. G., Jia, S. L., Jentzen, W., and Medforth, C. J. (1998) Nonplanar porphyrins and their significance in proteins. *Chem. Soc. Rev. 27*, 31−41.
(56) Bennett, M., Krah, A., Wien, F., Garman, E., McKenna, R., Sanderson, M., and Neidle, S. (2000) A DNA-porphyrin minor-groove complex at atomic resolution: The structural consequences of porphyrin ruffling. *Proc. Natl. Acad. Sci. U.S.A. 97*, 9476−9481.
(57) Kruk, N. N., Dzhagarov, B. M., Galievsky, V. A., Chirvony, V. S., and Turpin, P. Y. (1998) Photophysics of the cationic 5,10,15,20-tetrakis(4-N-methylpyridyl) porphyrin bound to DNA, poly(dA-dT)$_2$ and poly(dG-dC)$_2$: Interaction with molecular oxygen studied by porphyrin triplet-triplet absorption and singlet oxygen luminescence. *J. Photochem. Photobiol., B 42*, 181−190.
(58) Verlhac, J. B., Gaudemer, A., and Kraljic, I. (1984) Water-soluble porphyrins and metalloporphyrins as photosensitizers in aerated aqueous-solutions. 1. Detection and determination of quantum yield of formation of singlet oxygen. *Nouv. J. Chim. 8*, 401−406.
(59) Harriman, A., Porter, G., and Walters, P. (1983) Photooxidation of metalloporphyrins in aqueous-solution. *J. Chem. Soc., Faraday Trans. 1 79*, 1335−1350.
(60) Kalyanasundaram, K., and Neumannspallart, M. (1982) Photophysical and redox properties of water-soluble porphyrins in aqueous-media. *J. Phys. Chem. 86*, 5163−5169.
(61) Rogers, J. E., Nguyen, K. A., Hufnagle, D. C., McLean, D. G., Su, W. J., Gossett, K. M., Burke, A. R., Vinogradov, S. A., Pachter, R., and Fleitz, P. A. (2003) Observation and interpretation of annulated porphyrins: Studies on the photophysical properties of meso-tetraphenylmetalloporphyrins. *J. Phys. Chem. A 107*, 11331−11339.
(62) Schweitzer, C., and Schmidt, R. (2003) Physical mechanisms of generation and deactivation of singlet oxygen. *Chem. Rev. 103*, 1685−1757.
(63) Abdel-Shafi, A. A., and Wilkinson, F. (2002) Electronic to vibrational energy conversion and charge transfer contributions during quenching by molecular oxygen of electronically excited triplet states. *Phys. Chem. Chem. Phys. 4*, 248−254.
(64) Grewer, C., and Brauer, H. D. (1994) Mechanism of the triplet-state quenching by molecular-oxygen in solution. *J. Phys. Chem. 98*, 4230−4235.
(65) Turro, N. J., Ramamurthy, V., and Scaiano, J. C. (2009) *Principles of molecular photochemistry, an introduction*, Chapter 7, University Science, Sausalito, CA.
(66) Choi, J., and Majima, T. (2011) Conformational changes of non-B DNA. *Chem. Soc. Rev. 40*, 5893−5909.
(67) Ma, D. L., He, H. Z., Leung, K. H., Chan, D. S. H., and Leung, C. H. (2013) Bioactive luminescent transition-metal complexes for biomedical applications. *Angew. Chem., Int. Ed. 52*, 7666−7682.
(68) Ma, D. L., He, H. Z., Leung, K. H., Zhong, H. J., Chan, D. S. H., and Leung, C. H. (2013) Label-free luminescent oligonucleotide-based probes. *Chem. Soc. Rev. 42*, 3427−3440.
(69) Keane, P. M., and Kelly, J. M. (2011) Triplet-state dynamics of a metalloporphyrin photosensitiser (PtTMPyP4) in the presence of halides and purine mononucleotides. *Photochem. Photobiol. Sci. 10*, 1578−1586.